



Effect of annealing treatment on the structure and properties of the nanograined TiN coatings produced by ultrasonic-based coating process

S. Romankov^{a,*}, Y. Hayasaka^b, N. Hayashi^a, E. Kasai^a, S. Komarov^c

^a Institute of Multidisciplinary Research for Advanced Materials, Tohoku University, 2-1-1 Katahira, Aobaku, Sendai 980-8577, Japan

^b High Electron Voltage Microscope Laboratory, Tohoku University, Sendai 980-8577, Japan

^c NRDC, Nippon Light Metal Co. Ltd, Shizuoka 421-3291, Japan

ARTICLE INFO

Article history:

Received 28 July 2008

Received in revised form 19 October 2009

Accepted 20 October 2009

Available online 29 October 2009

Keywords:

Coating materials

Nanostructured materials

Nitride materials

Mechanical alloying

ABSTRACT

An ultrasonic mechanical coating and armouring (UMCA) process was used for the deposition of the nanograined TiN coatings. During the UMCA process, the substrate surface was subjected to high-energy ball impacts. The repeated substrate-to-ball collisions made the precoated TiN particles cold weld to each other and to the substrate. The UMCA method allows nanograined TiN coatings to be produced on different substrates in a short time at room temperature in an ambient atmosphere. Under the applied compressive loading, the substrate became strongly deformed. The grain refinement occurred and many randomly orientated nanosized grains developed near the substrate surface. Annealing treatment in temperatures ranging between 200 °C and 600 °C improved adhesion of the coatings and increased hardness. The nanoparticles had a tendency to consolidate with increasing annealing temperature. The growth of crystallites started at 400 °C. After annealing at 600 °C, a solid state reaction between Al and TiN leads to the formation of a new phase that could be intermetallic compound AlTi₃.

© 2009 Elsevier B.V. All rights reserved.

1. Introduction

The ultrasonic mechanical coating and armouring (UMCA) process may provide a simple and effective procedure for the coating fabrication [1–4]. One of the attractive features of this process is that it can be carried out at room temperature and atmospheric pressure, and the combined effects of surface modification (such as cold-hardening), mechanical activation, and nanocrystallization of substrates can be achieved by this coating treatment in just one operation. Fig. 1 shows a schematic illustration of the UMCA method. The chamber is attached to an ultrasonic transducer powered with a high-frequency generator at a resonant frequency above 20 kHz. Resonant high-amplitude vibrations accelerate the balls towards the substrate surface and this induces high-frequency ball-to-substrate collisions, as schematically shown in Fig. 1. In order to fabricate uniform coatings, the substrates are first pre-coated with an ethanol suspension of the particles deposited. Then, the precoated surface is treated with the balls. The balls strike the substrate at a high velocity of about 10 m/s and high-frequency of about 100 times per s and cm². The repeated ball-to-substrate collisions cold weld particles to the substrate surface. Cold welding particles under dynamic loading are achieved in a short

time of about 1 min at room temperature in an ambient atmosphere.

The UMCA have been used for deposition of Ti–Al and LaPO₄ coatings [2,3]. Our next step was to apply these methods for the deposition of hard coatings. The TiN coatings were chosen as a representative example. Our first attempt revealed that nanostructured TiN coating with good adhesion can be formed by UMCA method on the steel, Ti, and Al substrates [4]. The properties of the coatings should be improved. For that purpose annealing treatment of the nanostructured TiN coating was carried out. This paper reports the effect of the annealing treatment on the structure and properties of the TiN coatings fabricated by UMCA method.

2. Experimental procedures

The polished SUS 304 stainless steel, Ti and Al samples were used as the substrates. The TiN powder provided by Wako Corp., Japan, was used as raw materials for UMCA deposition. The average particle size of TiN was 50 nm. However, the coarse particles were occasionally observed. The volume fraction of the latter did not exceed 20%. The substrates were first precoated with a TiN particle-containing ethanol suspension and dried up. Then, the surface precoated with the TiN particles was treated using balls through the UMCA process at room temperature under ambient pressure. ZrO₂ balls with diameter of 3 mm were used to avoid iron contamination. The duration of ball treatment was 6 min. After that, as-synthesized samples were annealed in Ar atmosphere at 200 °C, 400 °C and 600 °C and were then cooled in the furnace. In all cases, the annealing time was 1 h.

The sample phase composition was studied by X-ray diffraction (XRD) analysis using a Rigaku diffractometer with CuK_α radiation in the 2θ range of 30–150. The XRD analysis was also used to determine the average crystallite size *D* on the basis of the Hall–Williamson analysis of TiN peak broadening. The coating thick-

* Corresponding author.

E-mail address: romankovs@mail.ru (S. Romankov).

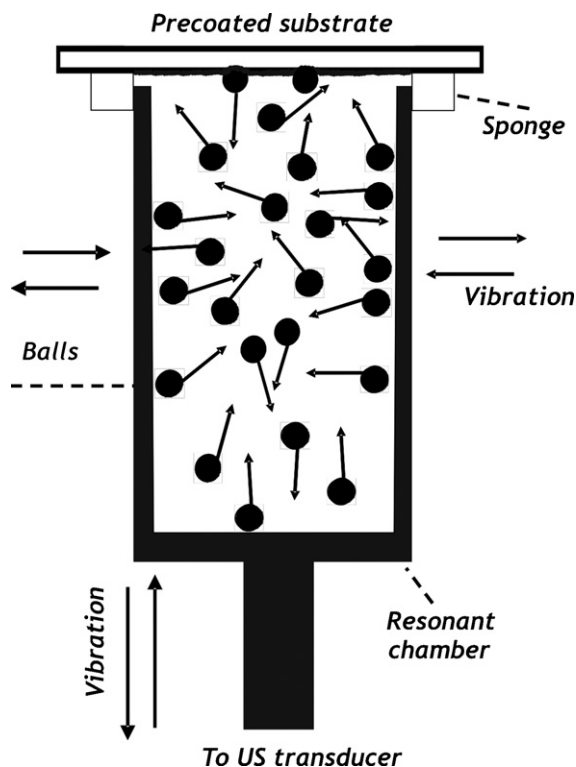


Fig. 1. Schematic illustration of the UMCA process.

ness was determined from the cross sections using a Hitachi S-4100L scanning electron microscope (SEM). JEOL Cross Section Polisher SM-09010 was employed for the preparation of the cross sections. For transmission electron microscopy (TEM), specimens were cut, ground, dimpled, and finally ion-thinned at low tem-

peratures. The TEM specimens were examined in a JEM-3010 TEM operated at 300 kV.

Revetest Xpress Scratch Tester (CMS Instruments) was used to evaluate the adhesion of the TiN coatings. The tests were carried out in a manner that the load applied on the diamond tip (tip radius was 200 μm) was continuously increased, while the tip was moving with a constant speed. The loading rate and speed were 100 N/min and 10 mm/min, respectively. The critical loads, at which the coating was fully delaminated, were defined by optical microscope and acoustic emission.

The microhardness was measured on the surface of the coatings. The measurements were carried out using an automated load Akashi Hardness Testing Machine at load of 50 g for duration of 10 s. Ten measurements were taken across each sample to obtain the average value of microhardness. The microhardness reported in this work may have a deviation of 3% from the absolute value.

3. Results and discussion

The repeated ball-to-substrate collisions made the precoated TiN particles cold weld to each other and to the substrate. The coating thickness was around 5 μm . Fig. 2a and b shows the typical cross-sectional TEM images of the TiN coatings. At the interface the TiN particles and substrate coalesced and formed a bulk material, which made the interface ill separated. It was especially noticeable on the Ti substrate (Fig. 2a). In the case of Al substrate, the TiN particles could be embedded in the substrate as individual TiN particles (Fig. 2b). Under the ball collisions, the substrates were heavily strained in a rather inhomogeneous manner. The grain refinement occurred and randomly orientated nanosized grains developed near the substrate surface as it was observed after mechanical attrition treatment or ultrasonic shot peening [5–7]. The coating structure may be represented as chains of the TiN particles cold welded on the substrate (Fig. 2c). The nanoparticles have sizes in the range of a few tenths of nanometres, similar to the original TiN particles. It signifies that under the ball collisions the particle consolidated quickly and they did not have time to increase their grain size. The consolidation of the particles occurred locally (Fig. 2c).

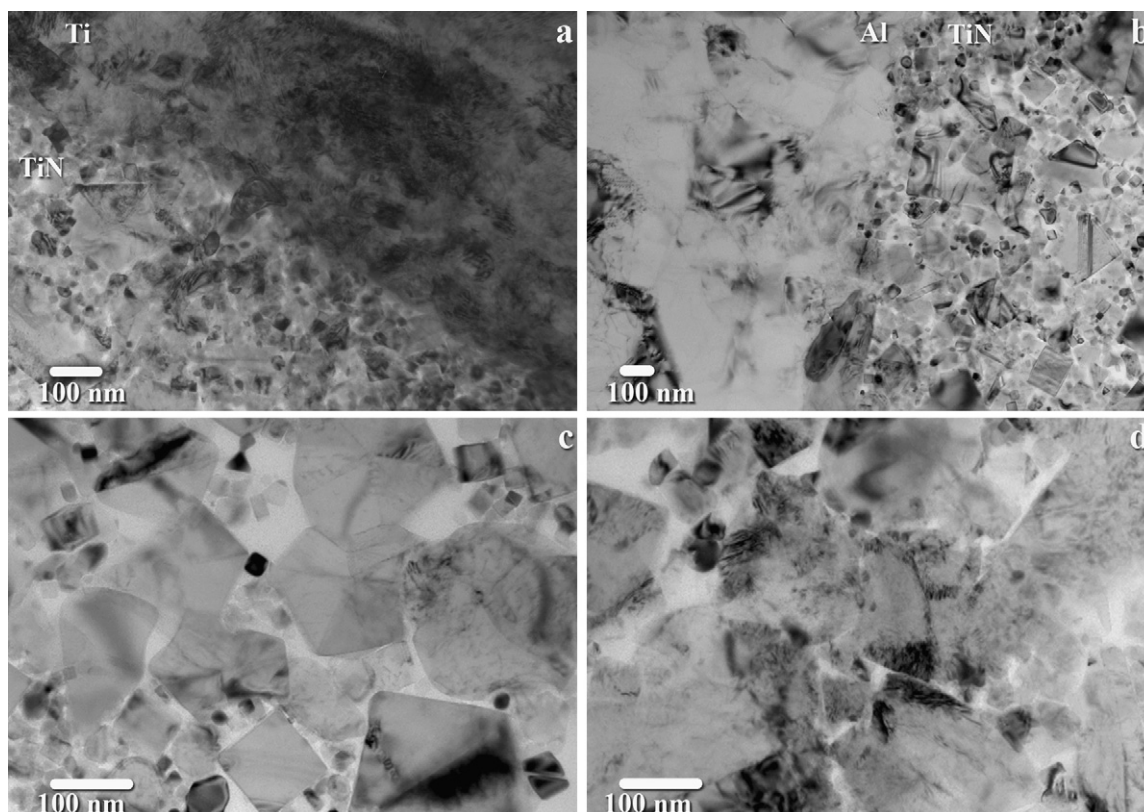


Fig. 2. Cross-sectional TEM micrographs, showing structure of the TiN coatings: (a) on the Ti substrate; (b) on Al substrate; (c) typical chain of the TiN particles cold welded on the Al substrate; (d) consolidation of the TiN particles on the Al substrate after annealing at 400 °C.

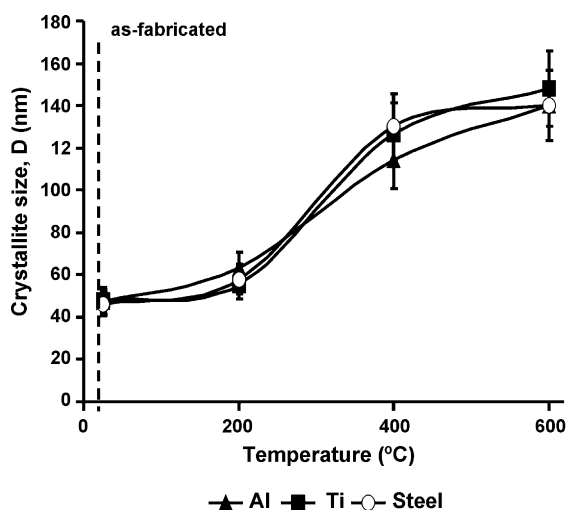


Fig. 3. Size of the TiN crystallites as a function of the annealing treatment.

The coating did not consolidate into the fully densified compact. It might be expected that the full densification of the UMCA-coatings into the bulk material could improve properties. For that purpose annealing treatment of the coatings was carried out.

Fig. 3 shows the growth of the TiN crystallites as a function of annealing temperature. A similar tendency for growth TiN crystallites was observed on all substrates. The greater grain growth of the TiN particles seems to occur above 400 °C. Annealing at relatively low temperature caused serious grain growth, since large amount of stored energy was in the form of grain boundaries. A representative example of grain coarsening after annealing at 400 °C is shown in Fig. 2d.

Fig. 4 shows a series of XRD patterns indicating the diffraction peak development after annealing, using the Al substrate as an example. For the Ti and steel substrates, when the annealing temperature increased, the widths of the diffraction peaks decreased, implying that the crystallites became larger in size and lattice strains lowered. No other phases were found to have formed after annealing of the steel and Ti substrates. In the case of the Al substrate, the intensities of the TiN peaks lowered after annealing at 400 °C (Fig. 4). Also, the relative changes in intensities of the Al diffraction peaks took place. After annealing at 600 °C, the intensities of the TiN lines almost decreased by half compared with as-fabricated sample. New diffraction lines denoted as X in Fig. 4 were observed in the XRD pattern. Moreover, the intensity of the most Al peaks was much weaker than that annealed at 400 °C except the peaks at 2θ diffraction angles of 44.6° and 65.1°. These diffraction peaks are likely to be a combination of two diffraction lines: Al and new phase. The diffraction lines of a new phase can be attributed to an intermetallic compound AlTi₃. The formation of the AlTi₃ phase has been observed in Ref. [8]. According to Ref. [8], at first Al diffused into TiN, occupying Ti sites with consequent formation of nitrogen vacancies. Further heating in presence of aluminum leads to the formation of AlTi₃. Qualitatively, the changes in the diffraction profiles after annealing above 400 °C in our case suggest that a solid state reaction between Al and TiN leads to the formation of a new phase.

Fig. 5a shows the results of scratch test of the coatings as a function of the annealing temperature. The figure gives the changes in the critical loads of the annealed TiN coatings with respect to the as-fabricated TiN coatings. The temperature dependence of the critical load implies that the coating adhesion increased with increasing annealing temperature. It could be related to the development of the interdiffusion process at the substrate/coating interface during annealing. Interdiffusion of elements between substrate and

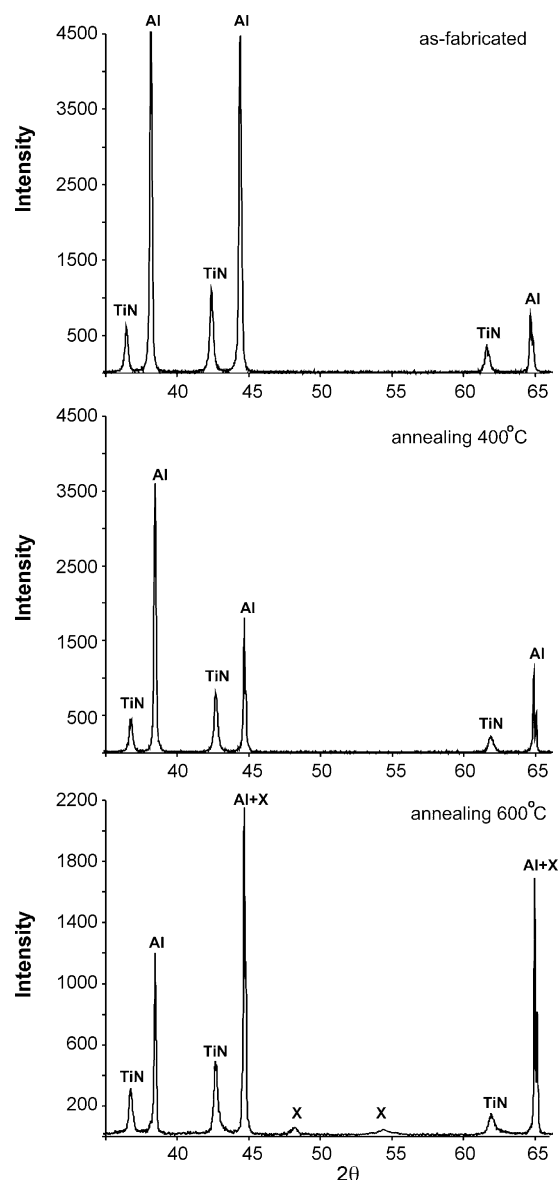


Fig. 4. XRD patterns of the TiN coatings on the Al substrate, showing development of the diffraction peaks after annealing treatment. New lines are marked as X could be attributed to an intermetallic compound AlTi₃. Note the different scales in the plots.

coating could enhance bonding. Besides, the TiN particles started to form stronger bonds with temperature because of interparticle diffusion. A high density of grain boundaries at the interface and a large amount of different defects produced by compressive loading promoted the diffusion. Increase in the value of the critical load was much greater for the TiN coating on the Al substrate than that on the Ti and steel ones. It is obvious that the diffusion rate for Al in temperatures ranging between 200 °C and 600 °C was higher than that for Ti and steel, so the value of the critical load for the coating fabricated on the Al substrate could increase more significantly. An increase in adhesion could be also concerned with the structural changes at the interface.

The microhardness measurements indicated a significant strengthening of the steel surface coated with TiN after annealing treatment (Fig. 5b). However, the microhardness of the Ti and Al samples decreased after annealing at 200 °C and 400 °C, and increased slightly after treatment at 600 °C. The microhardness measurements were carried out at load of 50 g. At that load the

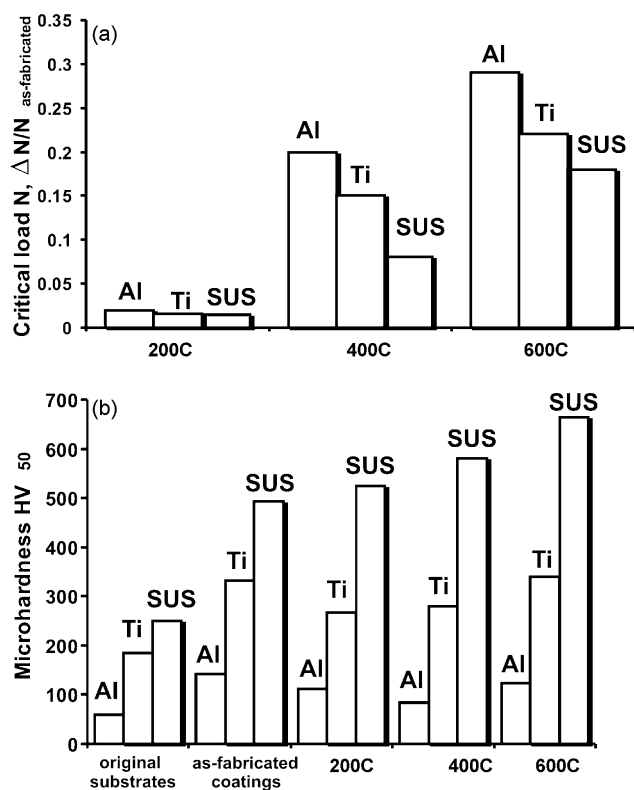


Fig. 5. Properties of the TiN coatings as functions of the annealing treatment: (a) changes in the critical loads of the annealed TiN coatings with respect to the as-fabricated TiN coatings; (b) microhardness.

effect of substrate cannot be ignored because the thickness of the coatings was around 5 μm . Under the ball collisions, the substrate became strongly deformed. The strain introduced into the surface, the grain refinement, and crystalline imperfections resulted in cold-hardening of the substrates. Annealing treatment led to stress

relaxation and grain growth, and the value of the surface microhardness of the Ti and Al substrates decreased faster than the steel one. Increasing microhardness after treatment at 600 °C could be caused by consolidation of the TiN coatings. Besides, in the case of the Al substrate, the formation of the new phase at the interface upon heating up to 600 °C could result in strengthening of the surface.

4. Summary

A UMCA method allows nanograined TiN coatings to be produced on different substrates in a short time at room temperature in an ambient atmosphere. The TiN particles consolidated quickly and they did not have time to increase their grain size. Under the applied compressive loading, the substrate became strongly deformed. The grain refinement occurred and many randomly orientated nanosized grains developed near the substrate surface. Annealing treatment in temperatures ranging between 200 °C and 600 °C improved the coating adhesion and microhardness properties. It is caused by structural changes of the coatings. The nanoparticles had a tendency to consolidate with increasing annealing temperature. The growth of crystallites started at rather low temperature, because of the high atom mobility achieved due to a high density of the grain boundaries.

References

- [1] Patent JP 2007-1977617.
- [2] S.V. Komarov, S.H. Son, N. Hayashi, S.D. Kaloshkin, O.V. Abramov, E. Kasai, Surf. Coat. Technol. 201 (2007) 6999–7006.
- [3] S. Romankov, S.V. Komarov, N. Hayashi, S. Ueno, S. Kaloshkin, E. Kasai, Surf. Coat. Technol. 202 (2008) 4285–4290.
- [4] S. Romankov, S.V. Komarov, E. Vdovichenko, Y. Hayasaka, N. Hayashi, E. Kasai, Int. J. Refract. Met. Hard Mater. 27 (2009) 492–497.
- [5] K. Lu, J. Lu, Mater. Sci. Eng. A 375–377 (2004) 38–45.
- [6] X.L. Wu, N.R. Tao, Q.M. Wei, P. Jiang, J. Lu, K. Lu, Acta Mater. 55 (2007) 5768–5779.
- [7] X. Wu, N. Tao, Y. Hong, B. Xu, J. Lu, K. Lu, Acta Mater. 50 (2002) 2075–2084.
- [8] E.K. Tentardini, C. Aguzzoli, M. Castro, A.O. Kunrath, J.J. Moore, C. Kwietniewski, I.J.R. Baumvol, Thin Solid Films 516 (2008) 3062–3069.